Excess of NPM-ALK oncogenic signaling promotes cellular apoptosis and drug dependency

Excess of NPM-ALK oncogenic signaling promotes cellular apoptosis and drug dependency

Monica Ceccon[1*], Maria Elena Boggio Merlo[2,3*], Luca Mologni[1], Teresa Poggio[2,3], Lydia M. Varesio[2,3], Matteo Menotti[2,3], Silvia Bombelli[1], Roberta Rigolio[4], Andrea D. Manazza[2,3], Filomena Di Giacomo[2,3], Chiara Ambrogio[5], Giovanni Giudici[6], Cesare Casati[7], Cristina Mastini[2,3], Mara Compagno[2,3,8], Suzanne D. Turner[9], Carlo Gambacorti-Passerini[1,10,#], Roberto Chiarle [2,3,8,#], Claudia Voena[2,3].

[1]Department of Health Science, University of Milano-Bicocca, Monza, Italy; [2]Department of Molecular Biotechnology and Health Sciences, University of Torino, Torino, Italy; [3]Center for Experimental Research and Medical Studies (CERMS), Città della Salute e della Scienza, Torino, Italy; [4]Surgery and Translational Medicine department, University of Milano-Bicocca, Monza, Italy; [5]Molecular Oncology Program, Centro Nacional de Investigaciones Oncológicas, Madrid, Spain; [6]Tettamanti Research Centre, Pediatric Clinic, University of Milano-Bicocca, Monza, Italy; [7]MetaSystems s.l.r., Milano, Italy; [8]Department of Pathology, Children's Hospital and Harvard Medical School, Boston, USA; [9]Division of Molecular Histopathology, Addenbrooke's Hospital Cambridge, Cambridge, UK; [10]Section of Haematology, San Gerardo Hospital, Monza, Italy

* These authors equally contributed

Co-corresponding authors

Running title: Excess NPM-ALK signaling is toxic in ALCL

Corresponding authors:

Roberto Chiarle, M.D.

Department of Pathology, Children's Hospital Boston and Harvard Medical School

Enders 1116.1, 320 Longwood Ave, Boston, MA 02115

email: roberto.chiarle@childrens.harvard.edu

Phone: +1 (617) 919-2662

Fax: +1 (617) 730-0148

Carlo Gambacorti-Passerini

Department of Health Science, University of Milano-Bicocca

Via Cadore 48, Monza 20900, Italy

email: carlo.gambacorti@unimib.it

The authors declare no conflict of interests.

ABSTRACT

Most of Anaplastic Large Cell Lymphoma (ALCL) cases carry the t(2;5; p23;q35) that produces the fusion protein NPM-ALK. NPM-ALK deregulated kinase activity drives several pathways that support malignant transformation of lymphoma cells. We found that in ALK-rearranged ALCL cell lines NPM-ALK was distributed in equal amounts between the cytoplasm and the nucleus. Only the cytoplasmic portion was catalytically active in both cell lines and primary ALCL, whereas the nuclear portion was inactive due to heterodimerization with NPM. Thus, about 50% of the NPM-ALK is not active and sequestered as NPM-ALK/NPM heterodimers in the nucleus. Overexpression or re-localization of NPM-ALK to the cytoplasm by NPM genetic knock-out or knock-down caused ERK1/2 increased phosphorylation and cell death through the engagement of an ATM/Chk2 and γH2AX mediated DNA damage response. Remarkably, human NPM-ALK amplified cell lines resistant to ALK tyrosine kinase inhibitors (TKIs) underwent apoptosis upon drug withdrawal as a consequence of ERK1/2 hyperactivation. Altogether, these findings indicate that an excess of NPM-ALK activation and signaling induces apoptosis via oncogenic stress responses. A “drug holiday” where the ALK TKI treatment is suspended could represent a therapeutic option in cells that become resistant by NPM-ALK amplification.

Keywords: Anaplastic Large Cell Lymphoma, NPM-ALK, TKI resistance, oncogenic stress.

INTRODUCTION

Recurrent genetic alterations of the Anaplastic Lymphoma Kinase (ALK) gene on chromosome 2 have been reported in different hematological and solid tumors[1, 2]. The t(2;5) is by far the most frequent translocation in Anaplastic Large Cell Lymphoma (ALCL) involving the nucleophosmin (NPM1) gene as a partner of translocation[1, 3]. Several other partner genes have been described in ALCL and other tumors[2]. All ALK fusion partners contain domains that allow the dimerization of the fusion chimera and the activation of the ALK kinase. NPM-ALK spontaneously dimerizes through the NPM1 oligomerization domain, trans-phosphorylates the kinase domain and activates downstream pathways that sustain lymphoma cell proliferation and survival. Cellular localization of ALK fusions depends on the fusion partner and the majority of ALK chimeras are entirely cytoplasmic[1, 4]. NPM-ALK is the only ALK chimera localized in both the cytoplasm and the nucleus. Previous works demonstrated that the cytoplasmic localization of ALK fusions is required for cellular transformation[5, 6], but no precise role has been yet assigned to the nuclear NPM-ALK or to the balance between its nuclear and cytoplasmic fractions. Understanding the functions of the NPM-ALK cell fractions could be exploited in the development of new therapeutic strategies that interfere with the physiological balance of NPM-ALK cytoplasmic and nuclear fractions in ALCL. Indeed, drugs that inhibit nuclear-cytoplasmic transport, so called selective inhibitors of nuclear export (SINE), have shown strong anti-tumoral activity in preclinical *in vitro* and *in vivo* studies and are currently in early-phase clinical trials for advanced hematological malignances and solid tumors[7, 8]. Moreover, previous studies demonstrated that in chronic myelogenous leukemia (CML) the combined use of imatinib, the selective inhibitor of the CML oncogenic driver kinase BCR-ABL, and leptomycin B, a “precursor” molecule of SINE, was more effective in killing cells than the inhibitor alone[9].

The recent discovery of specific ALK tyrosine kinase inhibitors (TKIs) has dramatically changed the way patients bearing ALK-rearranged tumors are treated[10, 11]. In ALK-rearranged non-small cell lung cancer (NSCLC) crizotinib, as well as next generation ALK TKI such as ceritinib, alectinib or brigatinib, have proven clinical efficacy[12-14]. Unfortunately, each TKI treatment is invariably associated with the development of TKI resistance and NSCLC relapse[15-18]. Similarly to NSCLC patients, crizotinib resistance occurs in a fraction of ALCL patients[19]. Understanding the mechanisms of ALK TKI resistance is critical to envision new treatment strategies to maximize the clinical benefits for ALK-rearranged ALCL patients. To date most of the data on the mechanisms of resistance to ALK TKI have been collected in NSCLC patients[20-23], whereas very few data are available for ALCL. Mechanisms of acquired resistance to ALK TKI in ALK-rearranged ALCL have been described mainly *in vitro* by our group and others, including single point mutations of the TK domain and amplification of the ALK fusion gene[24-28]. Amplification of the ALK fusion gene has also been described in ALK-rearranged NSCLC and leads to increased expression of the oncogenic ALK fusion that requires increasing dosage of ALK TKI to be treated. Overexpression of a driver oncogene as a mechanism of resistance to TKI has been also reported in CML patients treated with imatinib[29]. Remarkably, acute over-activation following imatinib suspension in BCR-ABL amplified imatinib-resistant cells induces apoptosis of resistant cells[29-31]. In another notable example, melanoma cells develop resistance to B-RAF inhibitors, and B-RAF TKI suspension in resistant cells induces cell toxicity mediated by an excess of B-RAF oncogenic signaling[32]. Similar observations have been described in a few other cancer models[33, 34]. Overall, these data indicate that an intermitting administration of a TKI could represent a therapeutic approach designed to overcome TKI resistance in different tumors.

In this study we show that NPM-ALK is equally distributed between the cytoplasm and the nuclear fractions, where nuclear NPM-ALK is inactive. This nuclear sequestration is critical

for optimal survival of ALCL cells because an excess of NPM-ALK signaling causes oncogenic toxicity by activation of the DNA damage response pathway. Consistently, NPM-ALK amplified ALCL cells that developed resistance to the TKI brigatinib underwent massive apoptosis upon TKI suspension because of an excess of NPM-ALK activation. Thus, periodic ALK TKI suspension, a so-called “drug holiday”, may represent an effective treatment for ALCL patients developing TKI resistance by ALK amplification.

RESULTS

NPM-ALK is equally localized in the cytoplasm and the nucleus of ALCL cells, but it is phosphorylated only in the cytoplasm.

NPM-ALK is by far the most frequent fusion in ALK-rearranged ALCL, yet the only one localized both in the cytoplasm and in the nucleus[1, 2]. Previous works demonstrated that the cytoplasmic localization of ALK fusions is needed for cell transformation, but never fully elucidated the role of the nuclear fraction[5, 6]. Therefore, we first analyzed NPM-ALK subcellular localization to better investigate the role of its nuclear fraction. We found that in all ALK-rearranged ALCL cell lines, NPM-ALK fusion is equally distributed between cytoplasm and nucleus, as previously reported in one cell line[5], but, surprisingly, only the cytoplasmic fraction is phosphorylated and thereby kinetically active (Fig. 1A). Consistently, a phospho-ALK (Y1604) antibody stained only the cytoplasm in primary ALK-rearranged ALCL indicating that the NPM-ALK nuclear fraction is not active (Fig. 1B). Thus, despite NPM-ALK is expressed in equal amounts in the cytoplasm and in the nucleus in ALCL cells, only the half cytoplasmic fraction of the total NPM-ALK protein is catalytically active.

Enforced expression of NPM-ALK in the nucleus does not transform cells.

In the NPM-ALK fusion, NPM1 is truncated by the t(2;5) translocation before the nuclear (NLS) and the nucleolar localization signals (NuLS)(Fig 1C). Thus, we reasoned that NPM-ALK can enter the nucleus only as a heterodimer with WT NPM1, and that these nuclear heterodimers are inactive because of lack of trans-phosphorylation. To test this hypothesis we first generated a fusion NPM-ALK construct containing the total NPM1 protein (NPM_{tot}-ALK) (Fig 1C). When expressed in 293T cells, NPM_{tot}-ALK localized entirely to the nucleus and the nucleolus due to the now conserved NPM1 NLS and NuLS, whereas NPM-ALK localized both in the cytoplasm and in the nucleus (Fig. 1D and Supplementary Fig. 1A-B). Next we tested the cell transformation potential of NPM_{tot}-ALK in two independent assays. First, we stably transduced NPM-ALK, the kinase dead mutant K210R (NPM-ALK^{KD}) and NPM_{tot}-ALK constructs into NIH3T3 cells and performed an anchorage-independent cell growth assay. NIH3T3 cells expressing the NPM_{tot}-ALK showed limited anchorage-independent growth with few colonies growing in soft-agar similar to the inactive NPM-ALK^{KD}, strikingly less than NIH3T3 cells expressing oncogenic NPM-ALK (Fig. 1E-F). Second, we used the murine interleukin-3 (IL-3) dependent pro-B cell line Ba/F3. In this assay, the ectopic expression of NPM-ALK enabled Ba/F3 cells to grow in absence of IL-3, whereas neither NPM-ALK^{KD} nor NPM_{tot}-ALK did (Fig. 1G-H). Overall, these results indicate that NPM-ALK is sequestered by WT NPM1 in the nucleus in an inactive, non phosphorylated form. However, should active NPM-ALK homodimers form in the nucleus by release of heterodimers, they would be still unable to transform cells because of a lack of signaling as the experiments with the NPM_{tot}-ALK fusion indicate.

In the absence of WT NPM1, NPM-ALK expression is localized to the cytoplasm but induces cell death.

To further elucidate the role of WT NPM1 in NPM-ALK oncogenic signaling, we transduced mouse embryonic fibroblasts (MEFs) that lack NPM1 ($NPM^{-/-}$ MEF) with retroviruses

expressing NPM-ALK, NPM-ALK^{KD} or NPM$_{tot}$-ALK. Because NPM$^{-/-}$ cells do not proliferate *in vitro* and acquire a senescent phenotype in the presence of p53, we used NPM$^{-/-}$/p53$^{-/-}$ double-deficient MEFs and p53$^{-/-}$ MEFs as controls for NPM1 expression[35]. In contrast to NIH3T3 cells and p53$^{-/-}$ MEFs, in NPM$^{-/-}$/p53$^{-/-}$ MEFs, NPM-ALK and the kinase dead NPM-ALK^{KD} were now localized only in the cytoplasm further confirming that, without NPM1, NPM-ALK homodimers cannot enter the nucleus and are localized to the cytoplasm (Fig. 2A-B). In NPM$^{-/-}$/p53$^{-/-}$ MEFs, cytoplasmic NPM-ALK was catalytically active (Fig. 2A right-top panels). NPM-ALK expression was well tolerated in p53$^{-/-}$ MEFs whereas, quite surprisingly, it induced apoptosis in NPM$^{-/-}$/p53$^{-/-}$ MEFs with elevated activation of Caspase 3/7 (Fig. 2C-D). On the contrary, NPM$_{tot}$-ALK was largely nuclear in both NPM$^{-/-}$/p53$^{-/-}$ and p53$^{-/-}$ MEFs (Fig. 2A), but well tolerated as the NPM-ALK^{KD} (Fig. 2C-D). Cell localization experiments of NPM-ALK in NPM$^{-/-}$/p53$^{-/-}$ MEFs was not doable because of the massive apoptosis of the cells.

Thus, lack of NPM-ALK sequestration by WT NPM1 induces NPM-ALK accumulation in the cytoplasm resulting in cell apoptosis rather than transformation.

We next investigated the effects of knocking-down the endogenous WT NPM1 in ALK-rearranged ALCL cell lines. We transduced ALK-rearranged ALCL cell lines (SU-DHL-1, COST, TS and KARPAS 299) with two different shRNA targeting NPM1 (Fig. 3A and Supplementary Fig. 2A). The ALK-negative ALCL cell line, FEPD, was used as control. When NPM1 was knocked-down NPM-ALK phosphorylation increased compared to control cells, as we observed in NPM$^{-/-}$/p53$^{-/-}$ MEFs, likely due to the accumulation of NPM-ALK homodimers in the cytoplasm (Fig. 3A and Supplementary Fig. 2A). The accumulation of NPM-ALK in the cytoplasm led to apoptosis of ALK-rearranged ALCL cells (Fig 3B-D and Supplementary Fig. 2B). No apoptosis was observed after NPM1 silencing in control ALK- cell line FEPD (Fig. 3E).

These results indicate that in the absence of WT NPM1 the amount of phosphorylated NPM-ALK increases and that the excess of NPM-ALK signaling could be responsible for ALCL apoptosis.

Overexpression of NPM-ALK in the cytoplasm of ALCL cells induces apoptosis of lymphoma cells.

Prompted by these results, we investigated in more details the effects of NPM-ALK overexpression in ALK-rearranged ALCL cells. Four different ALK-rearranged ALCL cell lines (SU-DHL-1, COST, TS and KARPAS 299) and, as control, one ALK-negative lymphoma cell line (MAC-1) were first transduced with a TetON lentivirus and then with lentiviruses containing NPM-ALK or NPM-ALK^{KD} to create a doxycycline-inducible system to overexpress NPM-ALK or NPM-ALK^{KD} upon doxycycline addition (Fig. 4A and Supplementary Fig. 3A and 4A). Overexpression of NPM-ALK in ALK-rearranged cells was mainly localized to the cytoplasm and caused a marked increase in the amount of phosphorylated NPM-ALK (Fig. 4B). Although ALK-rearranged ALCL cells are strongly dependent on ALK kinase activity and signaling for their viability and proliferation, overexpression of NPM-ALK caused a significant increase in apoptosis and activation of caspases 3 and 7 within 48-72 hours after doxycycline induction (Fig. 4C-F and Supplementary Fig. 3B-C). Similar effects were observed by ectopic expression of NPM-ALK in ALK-negative lymphoma cells (Supplementary Fig. 4B).

Consistent with the *in vitro* results, overexpression of NPM-ALK in ALK-rearranged ALCL cells completely impaired cell growth *in vivo*. Indeed, no tumors were detected in s.c. xenografts of SU-DHL-1 and COST after overexpression of NPM-ALK (Fig. 4G-H).

Overall, these data indicate that higher expression levels of NPM-ALK in ALCL induce a relative increase of the cytoplasmic portion likely because the stoichiometric balance between NPM1 and NPM-ALK is altered. The increased cytoplasmic NPM-ALK results in

apoptosis and lymphoma growth impairment. Thus, sequestration of about 50% of the NPM-ALK fusion is necessary to maintain the proper amount of ALK signaling.

Overexpression of NPM-ALK causes DNA damage and accumulation of γH2AX microfoci through activation of the MAPK pathway.

Because oncogenes can induce apoptosis or senescence in response to DNA damage through replicative stress[36, 37], we asked whether an excess of NPM-ALK signaling would activate an oncogene-induced DNA damage response. We observed that ALK-rearranged ALCL cells overexpressing NPM-ALK displayed increased phosphorylation of the H2A histone family member X (γH2AX), a key protein in the DNA repair pathway, and accumulation of γH2AX microfoci in the nuclei at DNA double-strand breaks (DSBs) (Fig. 5A-C and Supplementary Fig. 5A-B and 6A). Overexpression of the NPM-ALK^{KD} did not cause formation of γH2AX microfoci (Fig. 5B-C and Supplementary Fig. 5A). Along with the accumulation of γH2AX, overexpression of NPM-ALK caused the localization of the p53 binding protein 1 (53BP1), another key player of the DNA damage response pathway, at foci overtime (Supplementary Fig. 7A-B).

As DNA damage generated by oncogenic stress results from the activation of one of two main DNA-damage checkpoint pathways, the ATM-Chk2 and the ATR-Chk1[38-40], we investigated whether the overexpression of NPM-ALK was associated with the activation of ATM/ATR/Chk pathway. We found that overexpression of NPM-ALK led mainly to the phosphorylation of Chk2 more than Chk1 or RPA32 (Fig.5D and Supplementary Fig. 5C, 6B and 8A). We also observed that excessive NPM-ALK signaling caused marked increase in the phosphorylation of the MAPK-ERK1/2 pathway, that has been described to mediate oncogenic stress (Fig. 5E and Supplementary Fig. 5B and 6A)[41]. To test whether hyper stimulation of cells through MAPK pathway was responsible for the DNA damage and phosphorylation of H2AX, we treated cells with a specific MEK inhibitor, CI-1040

(PD184352). SU-DHL-1 and COST cells were induced with doxycycline for 24h and concomitantly treated with CI-1040. In cells overexpressing NPM-ALK, the inhibition of MEK resulted in marked dephosphorylation of H2AX (Fig. 5E). Similarly, the ectopic expression of NPM-ALK in MAC-1 cells caused a strong activation of the MEK/ERK1/2 pathway and a marked increase in the phosphorylation of H2AX (Supplementary Fig. 8B). Inhibition of the MEK/ERK1/2 pathway decreased H2AX phosphorylation (Supplementary Fig. 8B). Thus, these data indicate that excess of NPM-ALK signaling induces a DNA damage response that is mediated by the MEK/ERK1/2 pathway.

KARPAS 299 resistant to the ALK TKI brigatinib (AP26113) overexpress NPM-ALK and are TKI dependent.

We and others recently described genomic amplification of the ALK locus as a mechanism of ALK TKI resistance [26, 28]. We reported three ALK-rearranged cell lines (K299AR300A, K299AR300B, K299AR300C) whose resistance to the ALK inhibitor brigatinib was mediated by genomic amplification that caused NPM-ALK overexpression (Fig. 6A)[26]. Interestingly, in all resistant cell lines overexpressed NPM-ALK was mainly localized in the cytoplasm both in presence and in absence of the inhibitor, a finding in line with our data on ectopic overexpression of NPM-ALK (Fig. 4 and 6B). Surprisingly, these cell lines showed the highest proliferative rate not in the absence of ALK TKI, but in the presence of low doses (40nM) of brigatinib. Indeed, inhibitor dose-response curves showed an abnormal proliferative peak around 40nM brigatinib in NPM-ALK amplified ALCL but not in parental cells (Fig. 6C). The cells showed the same abnormal dose-response curves upon inhibition with other ALK TKIs (crizotinib, alectinib, ceritinib and ASP3026) or with a HSP90 inhibitor (17-AAG) that causes NPM-ALK down-regulation (Supplementary Fig. 9). Thus, these cell lines with amplified NPM-ALK not only were TKI resistant but also showed TKI dependency. Interestingly, in the presence of 40nM brigatinib, NPM-ALK phosphorylation

levels and downstream signaling, including ERK1/2 phosphorylation, were comparable to parental cell lines (Fig. 6B and D). Remarkably, upon drug withdrawal the cytoplasmic fraction of NPM-ALK in ALK amplified cell lines became highly phosphorylated, caused hyper-activation of ERK1/2 and led to oncogenic stress through phosphorylation of H2AX, in keeping with the data in ALK-rearranged ALCL cell lines overexpressing NPM-ALK (Fig. 6B and 6D). As a consequence apoptosis was induced dramatically after 72h of drug suspension (Fig. 6E). The same effect was observed in another ALK-rearranged cell line resistant to the ALK inhibitor ASP3026, SUPM2R1. We recently demonstrated that in this cell line TKI resistance was mediated by both ALK amplification and an ALK point mutation [25]. Also in this cell line, TKI withdrawal was followed by increased cell death (Supplementary Fig. 10). Overall these data indicate that in NPM-ALK amplified resistant ALCL cells the increased expression of NPM-ALK fusion results in accumulation of cytoplasmic NPM-ALK. In this condition, the excess ALK signaling is partially abrogated by low doses of ALK TKI resulting in ALK phosphorylation and ERK1/2 signaling comparable to the parental cells. However, upon ALK TKI suspension, the excess NPM-ALK signaling secondary to the ALK amplification induces an oncogenic stress response with DNA damage and apoptosis.

Long-term suspension of ALK TKI selects cells with restored sensitivity.

Based on these results, we envisioned a therapeutic approach to overcome resistance mediated by ALK amplification in ALCL. We grew parental KARPAS 299 and resistant cells in the presence or in the absence of brigatinib for five weeks. As expected, parental KARPAS 299 did not grow in presence of the drug (Fig. 7A, left-top panel). Of the three resistant cell lines, K299AR300B never grew in absence of the TKI, possibly consistent with their higher apoptosis and DNA damage response (Fig. 7A, left-bottom and Fig. 6D-E). In contrast, K299AR300A and K299AR300C, after an initial apoptotic response,

recovered in absence of the TKI (Fig7A. right panels). Remarkably, sensitivity to brigatinib was restored in these cells that recovered after TKI suspension (K299AR300A- and K299AR300C-; Fig. 7B-C). IC50 values for brigatinib of K299AR300A- and K299AR300C- were similar to the original for parental cells (6 and 7nM versus 3nM, Fig. 7C). Interestingly, in these cells, NPM-ALK overexpression was lost as its expression levels were again similar to the parental cell line (Fig. 7D). These results are in accordance with recent data reported by Amin et al on regression in mice of NPM-ALK amplified ALCL xenografts upon TKI treatment suspension [28]. These results suggest that ALK TKI resistance mediated by ALK amplification could be tamed by cycles of drug suspension, a so-called "drug holiday" where ALK amplified cells would die under an oncogenic stress-mediated DNA damage.

DISCUSSION

In the present work we demonstrated that the amount of cytoplasmic NPM-ALK in ALCL is critical for optimal lymphoma growth and survival. We showed that only half of the total NPM-ALK in ALCL is active in the cytoplasm in the form of homodimers, whereas WT NPM1 sequesters the other half in the form of inactive heterodimers. Therefore in NPM-ALK rearranged ALCL a critical stoichiometric equilibrium is reached between WT NPM1 and oncogenic NPM-ALK, and a perturbation of such equilibrium in either directions results in diminished cell growth and viability. A decrease of NPM-ALK expression or activity results in lymphoma cell cycle arrest and apoptosis, as it has now been demonstrated in preclinical models and in clinical trials with ALK TKI[19, 42-44]. In the present study we demonstrate that also an excess of NPM-ALK signaling is detrimental to ALCL growth by triggering an oncogene-induced stress response and apoptosis, and that nuclear sequestration of NPM-ALK is essential to maintain the optimal levels and to prevent an excess of ALK signaling.

Oncogenes trigger growth-promoting and anti-apoptotic signals for malignant transformation and outgrowth, but under certain conditions they can also initiate cellular programs that lead to apoptosis or senescence[36]. This phenomenon known as oncogenic stress is a common response to a cell replicative stress and DNA damage induced by the enforced proliferation caused by the deregulated oncogenic activity. Oncogenes activate an ATR/ATM-regulated DNA damage response network that delays or prevents cancer progression in early phase until this checkpoint is compromised by genetic alterations that often result in modification of the ATM-Chk2-p53 pathway[36, 38]. In ALCL, the p53 pathway is rarely inactivated by mutations[45], but it has been suggested that its activity is partially inactivated in an MDM2 and JNK-dependent manner[46]. Our data show that ALCL are still susceptible to apoptosis induced by an oncogenic stress generated by an excess of NPM-ALK signaling. When NPM-ALK was overexpressed or redirected to the cytoplasm after elimination of the nuclear sequestration by NPM1 knock-out, a DNA damage response was readily demonstrated by phosphorylation of Chk2 and formation of γH2AX and 53BP1 nuclear foci. Similarly to other oncogenes, the NPM-ALK oncogenic stress response was mediated by hyperactivation of MEK/ERK1/2 signaling[36, 47, 48].

In the present work we also asked whether these findings could be exploited for therapeutic purposes. Exciting advancements in the therapy of ALCL are seemingly at hand after the development of ALK TKI. Our group was the first to show that the first generation ALK TKI crizotinib is potently active in ALCL patients relapsed after standard cytotoxic therapy[19, 43]. However, a fraction of patients relapse under therapy for the development of resistance to ALK TKI.

Studies in few patients so far confirmed that mechanisms of resistance in ALCL are similar to those that occur in ALK-rearranged NSCLC. Most cases of resistance are mediated by point mutations in the ALK tyrosine kinase domain that affect the binding of the ALK TKI[19, 24, 27]. As an alternative mechanism, we recently demonstrated that resistance to the ALK

TKI brigatinib can also originate from amplification of the NPM-ALK gene so that an increased amount of NPM-ALK is produced by the resistant cells[26]. In these amplified ALCL cells, the stoichiometric balance between NPM-ALK and WT NPM1 is altered by an excess of NPM-ALK expression due to gene amplification. In these conditions, we demonstrated that releasing ALK inhibition by brigatinib suspension induces a rebound excess of ALK signaling identical to ALCL where NPM-ALK is overexpressed. This signaling includes hyperphosphorylation of ERK1/2 and γH2AX and results in cell apoptosis. Long-term culture of resistant KARPAS 299 cells in the absence of the ALK TKI resulted in the selection and outgrowth of cells that showed restored sensitivity to brigatinib. In those cell lines NPM-ALK overexpression was abrogated, consistently with data shown. Thus, in line with other cases of resistance, such as B-Raf, BCR-ABL, and others[31-34, 49], our data suggest that patients that have developed resistance to ALK TKI mediated by NPM-ALK amplification might benefit from cycles of administration and suspension of TKI treatment, the so called “drug holiday” therapy[50, 51]. Remarkably, while our manuscript was in preparation, a drug holiday approach for NPM-ALK amplified ALCL was also proposed by Amin et al. with experiments in xenograft mouse models[28]. However, they did not provide any molecular mechanisms to explain their findings, which we now provide in our work.

A second possible therapeutic application of our findings would involve the use of drugs that alter the nuclear import-export, thereby creating an unbalance between the amounts of nuclear and cytoplasmic NPM-ALK. In the case of NPM-ALK accumulation in the cytoplasm an oncogenic stress response would be activated. In contrast, should NPM-ALK nuclear sequestration increase, the active cytoplasmic fraction would decrease. In either cases cell viability would be affected as we showed in this study. To test this hypothesis, in preliminary experiments we tested the nuclear export inhibitor KPT330 on ALCL cells. KPT330 is currently in clinical trial for the treatment of acute leukemia [8, 52]. Treatment with

KPT330 resulted in a marked apoptosis of ALCL cells (Supplementary Fig. 11A). Remarkably, KTP330 synergized with crizotinib in the induction of apoptosis (Supplementary Fig. 11B-E). Increased sensitivity to crizotinib suggests that KPT330 might decrease the amount of active cytoplasmic NPM-ALK by impeding the nuclear export. More detailed studies on this combination therapy are currently under way in our laboratory.

In conclusion, our findings establish a novel concept of a critical balance of NPM-ALK signaling in ALCL cells. Exploiting the unbalance created by NPM-ALK amplification in TKI resistant ALCL by a period "drug holiday' could represent an additional therapeutic strategy for the treatment of ALK-rearranged ALCL.

MATERIALS AND METHODS

Cell lines and reagents

Human ALK-rearranged (TS, SU-DHL1, SUP-M2, KARPAS 299, JB6, SR-786 and DEL) and ALK negative (MAC-1) ALCL cell lines were obtained from the DSMZ (German collection of Microorganisms and Cell Cultures) collection. COST and FEPD cell lines were kindly provided by Dr. Lamant. Resistant cell lines KARPAS 299, K299AR300A, K299AR300B and K299AR300C, were selected and grown in the presence of brigatinib (AP26113) as previously described[26]. MEF $NPM^{-/-}p53^{-/-}$ and MEF $p53^{-/-}$ were kindly provided by Dr. Colombo.

The ALK TKI brigatinib (AP26113) was kindly provided by Ariad Pharmaceutical. Crizotinib was kindly provided by Pfizer, ceritinib (LDK-378) by Novartis, ASP3026 by Astellas, while alectinib (CH5424802), 17-AAG, CI-1040 (PD184352) and KPT330 were purchased from Selleck Chemicals. Idarubicin (IDA_HCl) and Puromycin were purchased by Sigma-Aldrich.

NPM-ALK constructs, virus preparation, cell infection and cell sorting.

Pallino vector expressing NPM-ALK or NPM-ALK^{K210R} were previously described[53]. NPM_{tot}-ALK construct was generated by PCR. The PCR product was cloned into PCRII vector using the T/A cloning technology (Invitrogen) and then cloned into pallino retroviral vector at HINDIII/XhoI sites.

For the TetON system, NPM-ALK and NPM-ALK^{K210R} were cloned into a modified pCCL vector containing the coding sequence of the EGFP-1 and the inducible bidirectional PBI-1 promoter that co-express the cloned gene and EGFP-1, as reporter.

Lentiviral shRNA clones targeting NPM were obtained from Sigma.

Retroviruses and lentiviruses were generated and cells were infected as previously described[53].

For the lentiviral-mediated inducible gene expression, cells were co-infected with pCCL lentiviruses and the rtTA regulator plasmid, according to the TetON strategy[54].

For cell sorting enrichment, cells were induced with 1ug/ml doxycycline hyciclate for 12h and sorted for GFP expression on a MoFlo High-Performance Cell Sorter (DAKO Cytomation). Cells were analyzed for GFP content on a FACSCalibur flow cytometer (Becton Dickinson) and the CELLQuest (tm) software (BD) was used for the data acquisition and analysis.

Cell apoptosis, caspase, proliferation and soft-agar assays

Apoptosis was measured by flow cytometry after staining with 200nM tetrametylrodamine methyl-ester (TMRM) or with annexin V-propidium iodide (PI) apoptosis detection kit (BD Biosciences), as previously described[53]. For caspase assay, the activity of caspase-3 and -7 was measured using Caspase-Glo® 3/7 Assay (Promega) and the multi-detection

system Glomax (Promega). Proliferation and soft-agar assays were performed as previously described[24].

Protein subcellular fractionation and immunoblotting

Cells were processed for the cytoplasm-nuclear fractionation by sequential step of lysis following NE-PER kit (Thermo Scientific) protocol. Total cell lysates were extracted as previoulsy described[53].

Immunohistochemistry and immunofluorescence

Immunohistochemical and immunofluorescence stainings were performed as previously described[53]. Coverslips were viewed using a Leica TCS SP2 laser-scanning confocal microscope driven by the Leica Confocal Software; the images were acquired at room temperature, by means of a 63X PL APO objective, numerical aperture 1.32. Brightfield images were acquired on a Leica DM IRE2 microscope using a DC300F camera and analyzed with the IM 50 software.

Immunoblotting and immunofluorescence antibodies

Primary antibodies used: anti-ALK (Zymed); anti-phospo-ALK (Y1604), anti-phospho-H2AX (S139), anti-phospho-p44/42 (T202/Y2049), anti-p44/42, anti-phospho-Chk1 (S345), anti-phospho-Chk2 (T68), anti-RPA32 (Cell Signaling Technology); anti-Chk1 (Novocastra); anti-Chk2 (Upstate); anti-phospho-RPA32 (S4/S8, Bethyl Laboratories); anti-βTubulin (Sigma); anti-actin (Sigma); anti-hnRNP A2/B1 (Abcam); anti-NPM (Invitrogen).

FISH analysis

FISH analysis on K299AR300A, AR300B and AR300C cell lines was previously described[26]. Amplified NPM-ALK quantification was performed using the Metafer Slide Scanning System (MetaSystems Hard & Software GmbH). The image acquisition and the

analysis of the cells were performed automatically by using the Metafer Slide Scanning System (MetaSystems Hard & Software GmbH), connected to the motorized microscope ZEISS Axio Imager.Z2 (Carl Zeiss). 3-channels images of a predefined area of the samples were acquired at a magnification of 40x. A “Z-stack” acquisition mode was used for the Red and Aqua channels, in order to provide a tridimensional evaluation of the corresponding FISH signals. The Red and Aqua FISH signals that resided inside the DAPI counterstain contour of the selected cells were identified and counted by a sophisticated spot-counting algorithm (based on Horn-Schunck algorithm). The ratio between the Red and Aqua values was calculated for every cell, and a medium overall ratio for all the analyzed cells was then calculated and graphically reported by the software.

In vivo tumor challenge

NOD-SCID mice (Charles River Laboratories Italia S.p.A) were inoculated s.c and measured as previously described[55]. Mice were handled and treated in accordance with European Community guidelines.

Statistical Analysis

Dose–response curves were analyzed using GraphPad Prism 5 software. IC50 indicates the concentration of inhibitor that gives half-maximal inhibition. Statistical significance was calculated with T-Student test. P values of <0.05 were considered significant. Unless otherwise noted, data are presented as means ± sd.

Acknowledgments

We would like to thank Maria Stella Scalzo for technical support, Dr. Emanuela Colombo for kindly providing mouse embryonic fibroblasts that lack NPM1 (MEF $NPM^{-/-}p53^{-/-}$) and control fibroblasts (MEF $p53^{-/-}$), Dr. Guido Serini for the use of his confocal microscopy unit at the Candiolo Cancer Institute – IRCCS, Torino, Italy. We also would like to thank ARIAD PHARMACEUTICAL, PFIZER, ASTELLAS and NOVARTIS that kindly provided all drugs used in this study.

This work was supported by the Regione Lombardia (ID14546A) to CGP and by grants FP7 ERC-2009-StG (Proposal No. 242965 - "Lunely") to RC; Associazione Italiana per la Ricerca sul Cancro (AIRC) grant IG-12023 to RC; Koch Institute/DFCC Bridge Project Fund to RC; Ellison Foundation Boston to RC; Worldwide Cancer Research Association (former AICR) grant 12-0216 to RC.

Supplementary Information accompanies the paper on the Oncogene website (http://www.nature.com/onc).

REFERENCES

1 Chiarle R, Voena C, Ambrogio C, Piva R, Inghirami G. The anaplastic lymphoma kinase in the pathogenesis of cancer. *Nature reviews Cancer* 2008; **8**: 11-23.

2 Hallberg B, Palmer RH. Mechanistic insight into ALK receptor tyrosine kinase in human cancer biology. *Nature reviews Cancer* 2013; **13**: 685-700.

3 Morris SW, Kirstein MN, Valentine MB, Dittmer KG, Shapiro DN, Saltman DL *et al*. Fusion of a kinase gene, ALK, to a nucleolar protein gene, NPM, in non-Hodgkin's lymphoma. *Science* 1994; **263**: 1281-1284.

4 Pulford K, Morris SW, Turturro F. Anaplastic lymphoma kinase proteins in growth control and cancer. *J Cell Physiol* 2004; **199**: 330-358.

5 Bischof D, Pulford K, Mason DY, Morris SW. Role of the nucleophosmin (NPM) portion of the non-Hodgkin's lymphoma-associated NPM-anaplastic lymphoma kinase fusion protein in oncogenesis. *Molecular and cellular biology* 1997; **17**: 2312-2325.

6 Mason DY, Pulford KA, Bischof D, Kuefer MU, Butler LH, Lamant L *et al*. Nucleolar localization of the nucleophosmin-anaplastic lymphoma kinase is not required for malignant transformation. *Cancer research* 1998; **58**: 1057-1062.

7 Etchin J, Sanda T, Mansour MR, Kentsis A, Montero J, Le BT *et al*. KPT-330 inhibitor of CRM1 (XPO1)-mediated nuclear export has selective anti-leukaemic activity in preclinical models of T-cell acute lymphoblastic leukaemia and acute myeloid leukaemia. *British journal of haematology* 2013; **161**: 117-127.

8 Walker CJ, Oaks JJ, Santhanam R, Neviani P, Harb JG, Ferenchak G *et al*. Preclinical and clinical efficacy of XPO1/CRM1 inhibition by the karyopherin inhibitor KPT-330 in Ph+ leukemias. *Blood* 2013; **122**: 3034-3044.

9 Vigneri P, Wang JY. Induction of apoptosis in chronic myelogenous leukemia cells through nuclear entrapment of BCR-ABL tyrosine kinase. *Nature medicine* 2001; **7**: 228-234.

10 Mologni L. Inhibitors of the anaplastic lymphoma kinase. *Expert opinion on investigational drugs* 2012; **21**: 985-994.

11 Pall G. The next-generation ALK inhibitors. *Current opinion in oncology* 2015; **27**: 118-124.

12 Kwak EL, Bang YJ, Camidge DR, Shaw AT, Solomon B, Maki RG *et al*. Anaplastic lymphoma kinase inhibition in non-small-cell lung cancer. *The New England journal of medicine* 2010; **363**: 1693-1703.

13 Shaw AT, Kim DW, Mehra R, Tan DS, Felip E, Chow LQ *et al*. Ceritinib in ALK-rearranged non-small-cell lung cancer. *The New England journal of medicine* 2014; **370**: 1189-1197.

14 Mologni L. Expanding the portfolio of anti-ALK weapons. *Transl Lung Cancer Res* 2015; **4**: 5-7.

15 Friboulet L, Li N, Katayama R, Lee CC, Gainor JF, Crystal AS *et al*. The ALK inhibitor ceritinib overcomes crizotinib resistance in non-small cell lung cancer. *Cancer discovery* 2014; **4**: 662-673.

16 Katayama R, Friboulet L, Koike S, Lockerman EL, Khan TM, Gainor JF *et al*. Two Novel ALK Mutations Mediate Acquired Resistance to the Next-Generation ALK Inhibitor Alectinib. *Clinical cancer research : an official journal of the American Association for Cancer Research* 2014; **20**: 5686-5696.

17 Choi YL, Soda M, Yamashita Y, Ueno T, Takashima J, Nakajima T *et al*. EML4-ALK mutations in lung cancer that confer resistance to ALK inhibitors. *The New England journal of medicine* 2010; **363**: 1734-1739.

18 Ignatius Ou SH, Azada M, Hsiang DJ, Herman JM, Kain TS, Siwak-Tapp C *et al*. Next-generation sequencing reveals a Novel NSCLC ALK F1174V mutation and confirms ALK G1202R mutation confers high-level resistance to alectinib (CH5424802/RO5424802) in ALK-rearranged NSCLC patients who progressed on

crizotinib. *Journal of thoracic oncology : official publication of the International Association for the Study of Lung Cancer* 2014; **9**: 549-553.

19 Gambacorti Passerini C, Farina F, Stasia A, Redaelli S, Ceccon M, Mologni L *et al*. Crizotinib in advanced, chemoresistant anaplastic lymphoma kinase-positive lymphoma patients. *Journal of the National Cancer Institute* 2014; **106**: djt378.

20 Katayama R, Lovly CM, Shaw AT. Therapeutic targeting of anaplastic lymphoma kinase in lung cancer: a paradigm for precision cancer medicine. *Clinical cancer research : an official journal of the American Association for Cancer Research* 2015; **21**: 2227-2235.

21 Katayama R, Shaw AT, Khan TM, Mino-Kenudson M, Solomon BJ, Halmos B *et al*. Mechanisms of acquired crizotinib resistance in ALK-rearranged lung Cancers. *Science translational medicine* 2012; **4**: 120ra117.

22 Doebele RC, Pilling AB, Aisner DL, Kutateladze TG, Le AT, Weickhardt AJ *et al*. Mechanisms of resistance to crizotinib in patients with ALK gene rearranged non-small cell lung cancer. *Clinical cancer research : an official journal of the American Association for Cancer Research* 2012; **18**: 1472-1482.

23 Voena C, Chiarle R. The battle against ALK resistance: successes and setbacks. *Expert opinion on investigational drugs* 2012; **21**: 1751-1754.

24 Ceccon M, Mologni L, Bisson W, Scapozza L, Gambacorti-Passerini C. Crizotinib-resistant NPM-ALK mutants confer differential sensitivity to unrelated Alk inhibitors. *Molecular cancer research : MCR* 2013; **11**: 122-132.

25 Mologni L, Ceccon M, Pirola A, Chiriano G, Piazza R, Scapozza L *et al*. NPM/ALK mutants resistant to ASP3026 display variable sensitivity to alternative ALK inhibitors but succumb to the novel compound PF-06463922. *Oncotarget* 2015; **6**: 5720-5734.

26 Ceccon M, Mologni L, Giudici G, Piazza R, Pirola A, Fontana D *et al*. Treatment Efficacy and Resistance Mechanisms Using the Second-Generation ALK Inhibitor AP26113 in Human NPM-ALK-Positive Anaplastic Large Cell Lymphoma. *Molecular cancer research : MCR* 2015; **13**: 775-783.

27 Zdzalik D, Dymek B, Grygielewicz P, Gunerka P, Bujak A, Lamparska-Przybysz M *et al*. Activating mutations in ALK kinase domain confer resistance to structurally unrelated ALK inhibitors in NPM-ALK-positive anaplastic large-cell lymphoma. *Journal of cancer research and clinical oncology* 2014; **140**: 589-598.

28 Amin AD, Rajan SS, Liang WS, Pongtornpipat P, Groysman MJ, Tapia EO *et al*. Evidence Suggesting That Discontinuous Dosing of ALK Kinase Inhibitors May Prolong Control of ALK+ Tumors. *Cancer research* 2015.

29 Gorre ME, Mohammed M, Ellwood K, Hsu N, Paquette R, Rao PN *et al*. Clinical resistance to STI-571 cancer therapy caused by BCR-ABL gene mutation or amplification. *Science* 2001; **293**: 876-880.

30 Tipping AJ, Mahon FX, Lagarde V, Goldman JM, Melo JV. Restoration of sensitivity to STI571 in STI571-resistant chronic myeloid leukemia cells. *Blood* 2001; **98**: 3864-3867.

31 Desplat V, Belloc F, Lagarde V, Boyer C, Melo JV, Reiffers J *et al*. Overproduction of BCR-ABL induces apoptosis in imatinib mesylate-resistant cell lines. *Cancer* 2005; **103**: 102-110.

32 Das Thakur M, Salangsang F, Landman AS, Sellers WR, Pryer NK, Levesque MP *et al*. Modelling vemurafenib resistance in melanoma reveals a strategy to forestall drug resistance. *Nature* 2013; **494**: 251-255.

33 Suda K, Tomizawa K, Osada H, Maehara Y, Yatabe Y, Sekido Y *et al*. Conversion from the "oncogene addiction" to "drug addiction" by intensive inhibition of the EGFR and MET in lung cancer with activating EGFR mutation. *Lung Cancer* 2012; **76**: 292-299.

34 Funakoshi Y, Mukohara T, Tomioka H, Ekyalongo RC, Kataoka Y, Inui Y *et al*. Excessive MET signaling causes acquired resistance and addiction to MET

inhibitors in the MKN45 gastric cancer cell line. *Investigational new drugs* 2013; **31**: 1158-1168.

35 Colombo E, Bonetti P, Lazzerini Denchi E, Martinelli P, Zamponi R, Marine JC *et al*. Nucleophosmin is required for DNA integrity and p19Arf protein stability. *Molecular and cellular biology* 2005; **25**: 8874-8886.

36 Halazonetis TD, Gorgoulis VG, Bartek J. An oncogene-induced DNA damage model for cancer development. *Science* 2008; **319**: 1352-1355.

37 Hills SA, Diffley JF. DNA replication and oncogene-induced replicative stress. *Current biology : CB* 2014; **24**: R435-444.

38 Smith J, Tho LM, Xu N, Gillespie DA. The ATM-Chk2 and ATR-Chk1 pathways in DNA damage signaling and cancer. *Advances in cancer research* 2010; **108**: 73-112.

39 Kastan MB, Bartek J. Cell-cycle checkpoints and cancer. *Nature* 2004; **432**: 316-323.

40 Medema RH, Macurek L. Checkpoint control and cancer. *Oncogene* 2012; **31**: 2601-2613.

41 Wei F, Yan J, Tang D. Extracellular signal-regulated kinases modulate DNA damage response - a contributing factor to using MEK inhibitors in cancer therapy. *Curr Med Chem* 2011; **18**: 5476-5482.

42 Piva R, Chiarle R, Manazza AD, Taulli R, Simmons W, Ambrogio C *et al*. Ablation of oncogenic ALK is a viable therapeutic approach for anaplastic large-cell lymphomas. *Blood* 2006; **107**: 689-697.

43 Gambacorti-Passerini C, Messa C, Pogliani EM. Crizotinib in anaplastic large-cell lymphoma. *The New England journal of medicine* 2011; **364**: 775-776.

44 Hapgood G, Savage KJ. The biology and management of systemic anaplastic large cell lymphoma. *Blood* 2015.

45 Rassidakis GZ, Thomaides A, Wang S, Jiang Y, Fourtouna A, Lai R *et al*. p53 gene mutations are uncommon but p53 is commonly expressed in anaplastic large-cell lymphoma. *Leukemia : official journal of the Leukemia Society of America, Leukemia Research Fund, UK* 2005; **19**: 1663-1669.

46 Cui YX, Kerby A, McDuff FK, Ye H, Turner SD. NPM-ALK inhibits the p53 tumor suppressor pathway in an MDM2 and JNK-dependent manner. *Blood* 2009; **113**: 5217-5227.

47 Bartkova J, Rezaei N, Liontos M, Karakaidos P, Kletsas D, Issaeva N *et al*. Oncogene-induced senescence is part of the tumorigenesis barrier imposed by DNA damage checkpoints. *Nature* 2006; **444**: 633-637.

48 Maya-Mendoza A, Ostrakova J, Kosar M, Hall A, Duskova P, Mistrik M *et al*. Myc and Ras oncogenes engage different energy metabolism programs and evoke distinct patterns of oxidative and DNA replication stress. *Mol Oncol* 2015; **9**: 601-616.

49 Dengler MA, Staiger AM, Gutekunst M, Hofmann U, Doszczak M, Scheurich P *et al*. Oncogenic stress induced by acute hyper-activation of Bcr-Abl leads to cell death upon induction of excessive aerobic glycolysis. *PloS one* 2011; **6**: e25139.

50 Sun C, Wang L, Huang S, Heynen GJ, Prahallad A, Robert C *et al*. Reversible and adaptive resistance to BRAF(V600E) inhibition in melanoma. *Nature* 2014; **508**: 118-122.

51 Koop A, Satzger I, Alter M, Kapp A, Hauschild A, Gutzmer R. Intermittent BRAF-inhibitor therapy is a feasible option: report of a patient with metastatic melanoma. *The British journal of dermatology* 2014; **170**: 220-222.

52 Das A, Wei G, Parikh K, Liu D. Selective inhibitors of nuclear export (SINE) in hematological malignancies. *Exp Hematol Oncol* 2015; **4**: 7.

53 Voena C, Conte C, Ambrogio C, Boeri Erba E, Boccalatte F, Mohammed S *et al*. The tyrosine phosphatase Shp2 interacts with NPM-ALK and regulates anaplastic lymphoma cell growth and migration. *Cancer research* 2007; **67**: 4278-4286.

54 Gossen M, Freundlieb S, Bender G, Muller G, Hillen W, Bujard H. Transcriptional activation by tetracyclines in mammalian cells. *Science* 1995; **268**: 1766-1769.

55 Martinengo C, Poggio T, Menotti M, Scalzo MS, Mastini C, Ambrogio C *et al*. ALK-Dependent Control of Hypoxia-Inducible Factors Mediates Tumor Growth and Metastasis. *Cancer research* 2014; **74**: 6094-6106.

Figure Legends

Figure 1. In ALCL cells NPM-ALK is equally distributed between the cytoplasm and the nucleus, but it is phosphorylated only in the cytoplasm. A) ALK-rearranged ALCL cells were collected and total cell lysates were processed for the cytoplasm-nuclear fractionation. Cytoplasmic and nuclear fractions were blotted with the indicated antibodies. B) Immunohistochemistry on ALCL tissue samples with anti-ALK or anti-pALK(Y1604) antibody (top panels). Immunofluorescence staining with anti-ALK or anti-pALK(Y1604) antibody in TS cells (red fluorescence) (bottom panels). C) NPM-ALK constructs. The different constructs were cloned in a retroviral vector, pallino, with the reporter gene GFP. NPM-ALK fusion protein and the kinase dead mutant (K210R) NPM-ALK^{KD} are indicated. The translocated counterpart of NPM contains the oligomerization domain (OD) at the N-terminal, but it looses the nuclear (NLS) and nucleolar localization signals (NuLS) at the C-terminal, as indicated. NPM$_{tot}$-ALK construct was created by PCR amplification in order to force NPM-ALK expression in the nucleus. In this construct the entire NPM coding sequence is fused to the C-terminal of ALK. D) Human 293T cells were transfected with the indicated DNA constructs and harvested after 24h. Immunohistochemistry with a specific anti-ALK antibody was performed on formalin-fixed and paraffin-embedded cells (D). E-F) NPM$_{tot}$-ALK does not transform cells. NIH3T3 cells were infected with pallino-NPM-ALK, NPM-ALK^{KD} or NPM$_{tot}$-ALK. Total cell lysates were blotted with the indicated antibodies (E). NIH3T3 cells infected with the indicated constructs were plated in soft agar and cultured for 3 weeks. Histograms represent the average numbers of colonies grown in soft agar (F). Data are from one of three independent experiments. G-H) Nuclear NPM$_{tot}$-ALK does not support a cytokine independent growth. IL-3 dependent Ba/F3 cells were stably transfected with NPM-ALK, NPM-ALK^{KD} or NPM$_{tot}$-ALK. Ba/F3 cells were collected in presence of IL-3 and blotted with the indicated antibodies (G). Three days after infection

Ba/F3 cells were grown in absence of IL-3 and the percentage of viable cells was checked by FACS analysis at the indicated time points (H) Data are from one of two independent experiments. Statistical significance was calculated by Student's t-test where ***P <0.0005.

Figure 2. **In the absence of WT NPM1, NPM-ALK is entirely localized in the cytoplasm and causes cell death**. $NPM^{-/-}/p53^{-/-}$ MEF and $p53^{-/-}$ MEF cells were infected with pallino-NPM-ALK, NPM-ALK^{KD} or NPM_{tot}-ALK retrovirus. The percentage of GFP+ cells was checked by FACS analysis. A) Immunofluorescence staining with a specific anti-ALK antibody or anti-pALK(Y1604) was performed (red fluorescence). Green fluorescence is the EGFP reporter protein encoded by transduced cells. Nuclei were stained with DAPI. Images were taken with the Leica Confocal microscope. B) Cells were collected and processed for the cytoplasm-nuclear fractionation. Cytoplasmic and nuclear fractions were blotted with the indicated antibodies. C-D) The percentage of apoptosis in $NPM^{-/-}/p53^{-/-}$ MEF and $p53^{-/-}$ MEF cells was measured by TMRM staining and FACS analysis (C). The activation of the caspase 3/7 was analysed using Caspase-Glo® 3/7 Assay (Promega) and the Glomax multi-detection system (D). Statistical significance was calculated by Student's t-test where **P <0.005; ****P <0.0001.

Figure 3. Knocking-down wild-type NPM1 increases apoptosis in ALK-rearranged ALCL cells. A) ALK-rearranged ALCL cell lines (SU-DHL-1, COST, TS) and the ALK negative cell line, FEPD, were infected with two shRNA targeting NPM. Infected cells were grown in presence of 1ug/ml puromycin for selection, then harvested and analysed by Western blot with the indicated antibodies. Total cell lysates were blotted with the indicated antibodies. B-E) The percentage of apoptosis cells was measured by TMRM staining and FACS analysis. Data are from one of two independent experiments. Statistical significance was calculated by Student's t-test where * P <0.05; ***P <0.0005.

Figure 4. In ALK-rearranged ALCL overexpression of NPM-ALK causes excess of NPM-ALK signaling and cell death *in vitro* and impairs cell growth *in vivo*. A) ALK-rearranged ALCL cells (SU-DHL-1 and COST) were infected with a doxycycline-inducible lentivirus espressing NPM-ALK or the kinase dead, NPM-ALK^{KD}. The percentage of GFP+ cells was checked by FACS analysis. Cells were cultured in absence/presence of doxycycline (1µg/ml) for 24h to induce the expression of the indicated constructs and total cell lysates were collected for Western blot analysis with the indicated antibodies. B) SU-DHL-1 and COST inducible cell lines were collected and processed for the cytoplasm-nuclear fractionation. Cytoplasmic and nuclear fractions were blotted with the indicated antibodies. C-F) Cells were cultured in presence/absence of doxycycline for 48h. Cell death was analysed by TMRM staining and FACS analysis (C-D) and caspase 3/7 activation was analysed using Caspase-Glo® 3/7 Assay (Promega) and the Glomax multi-detection system . Data are from one of three independent experiments. G-H) NOD-SCID mice were inoculated s.c in both flanks with 106 ALK-rearranged ALCL inducible cell lines (SU-DHL-1 and COST). Tumor growth was measured at the indicated time points. Statistical significance was calculated by Student's t-test where *P <0.05; **P <0.005; **** P <0.0001.

Figure 5. **NPM-ALK overexpression leads to ATM-Chk2 pathway activation and causes DNA damage and γH2AX microfoci accumulation in the nuclei at DNA double-strand breaks through the MAPK pathway.** SU-DHL-1 and COST were infected with a doxycycline-inducible lentivirus expressing NPM-ALK or NPM-ALK^{KD} and grown in presence of doxycycline (1µg/ml). A) Immunofluorescence staining with a specific anti-γH2AX (S139) antibody (red fluorescence) was performed. Nuclei were stained with DAPI.

Green fluorescence is the EGFP reporter protein encoded by the retrovirally transduced cells. B-C) Histograms represent the % of γH2AX positive microfoci in SU-DHL-1 (B) and COST (C) at 48h from induction with doxycycline. D) Cells were induced with doxycycline, harvested at the indicated time points and blotted with the indicated antibodies. E) SU-DHL-1 and COST inducible cell lines (NPM-ALK and NPM-ALK^{KD}) were grown in presence of doxycycline for 48h and treated with the MEK inhibitor CI-1040 (1μM) for 24h. Total cell lysates were immunoblotted with the indicated antibodies. Statistical significance was calculated by Student's t-test where ***P* <0.05; *****P*<0.0001.

Figure 6. Resistant KARPAS 299 cell lines resistant to brigatinib overexpress NPM-ALK and are TKI dependent. Resistant cell lines K299AR300A, K299AR300B and K299AR300C were obtained as reported in Methods. A) Quantification of NPM-ALK genomic amplification was performed by using the Metafer Slide Scanning System. Values are normalized on the probe specific for centromere of chromosome 2. B) KARPAS 299 TetOn were induced with doxycycline for 48h and collected for the cytoplasm-nuclear fractionation. K299AR300A, K299AR300B and K299AR300C were collected after 48h of brigatinib suspension and processed for the cytoplasm-nuclear fractionation. Cytoplasmic and nuclear fractions were blotted with the indicated antibodies. C) A dose-response curve in the presence of brigatinib was performed on K299AR300A, K299AR300B and K299AR300C cell lines. Cells were incubated for three days in the presence of the indicated brigatinib concentration, then they were incubated for 8 hours with ^{3}H-radiolabeled thymidine. Radioactive incorporation was evaluated and normalized on the untreated wells. D) Cells were plated in absence or in presence of 40nM brigatinib for 24 or 48 hours then harvested and blotted with the indicated antibodies. E) Cells were incubated for 72 hours with or w/o brigatinib [40nM]. Apoptosis was evaluated by annexinV-PI staining. Histograms represent the percentage of apoptotic (annV+, PI+) cells

for each analysed cell population. Statistical significance was calculated by Student's t-test where $^{**}P < 0.005$.

Figure 7. Long-term suspension of ALK TKI selects cells with restored sensitivity to brigatinib. K299AR300A, K299AR300B and K299AR300C and parental K299 cells were cultured in the presence or in the absence of 300nM brigatinib for five weeks. A) Cell viability was measured in the presence of 300nM brigatinib (black squared), upon drug withdrawal (white rhombi), or after a new administration of 300nM brigatinib (grey rhombi) is shown. B) Dose-response curve obtained by ^{3}H proliferation test on K299AR300A, K299AR300A-, K299AR300C and K299AR300C- starting from 1μM brigatinib dose. C) Corresponding IC_{50} values and RR index are summarized. D) NPM-ALK expression in K299AR300A, K299AR300A-, K299AR300C and K299AR300C- was assessed by western blot.

Figure 8. Effects of an excess of NPM-ALK signaling in ALK-rearranged ALCL cells. Schematic representation of NPM-ALK signaling in ALK-rearranged ALCL cells in conditions where WT NPM is knocked out or NPM-ALK is overexpressed. Lymphoma cells resistant to ALK TKI via NPM-ALK amplification are induced to apoptosis upon drug suspension (drug holiday).

Figure 1

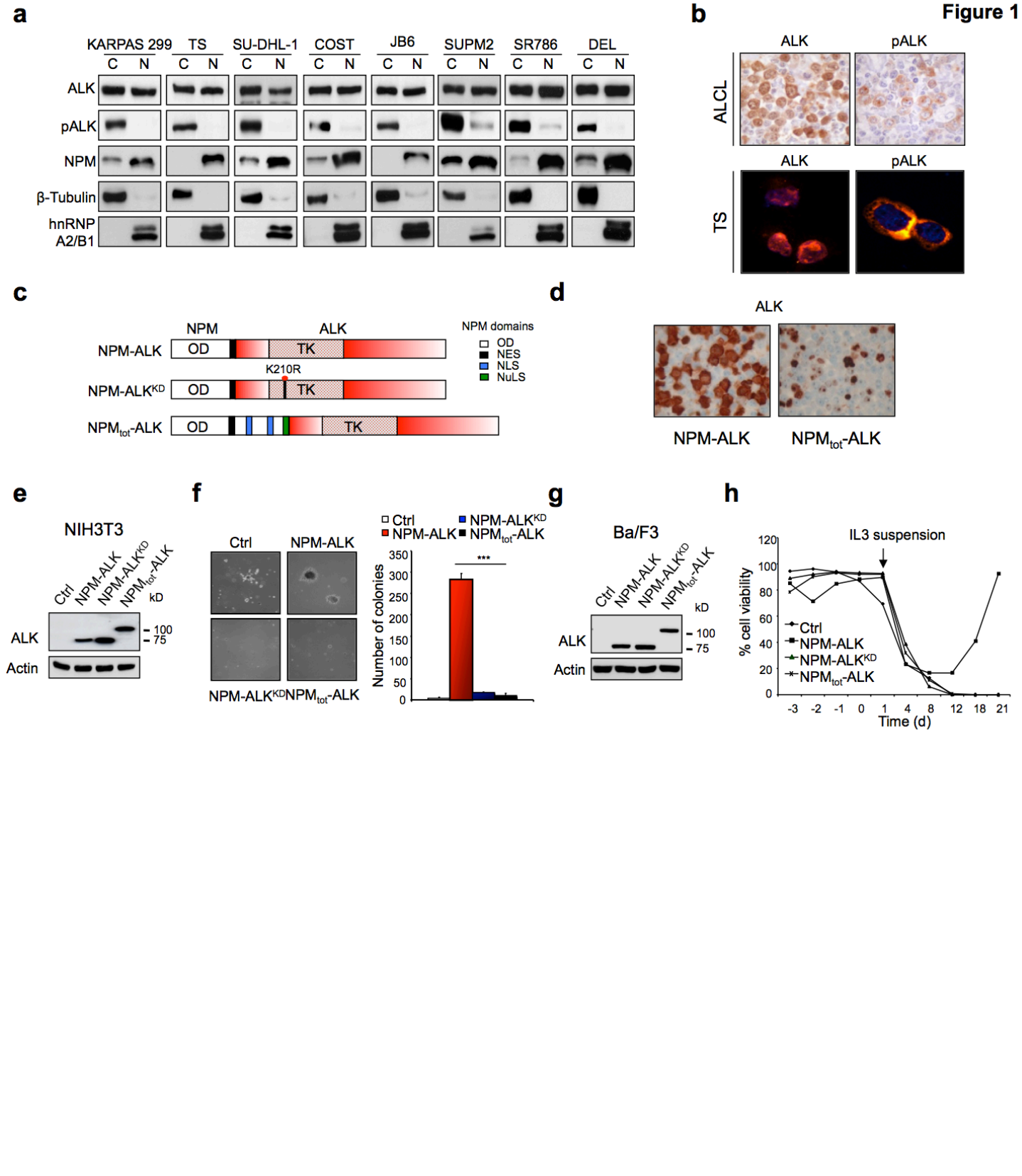
a
KARPAS 299
TS
SU-DHL-1
COST
JB6
SUPM2
SR786
DEL
C N
ALK
pALK
NPM
β-Tubulin
hnRNP A2/B1
b
ALK
pALK
ALCL
TS
c
NPM
ALK
NPM-ALK
OD
TK
K210R
NPM-ALK^KD
NPM_tot-ALK
NPM domains
OD
NES
NLS
NuLS
d
ALK
NPM-ALK
NPM_tot-ALK
e
NIH3T3
Ctrl
NPM-ALK
NPM-ALK^KD
NPM_tot-ALK
kD
ALK
Actin
100
75
f
Ctrl
NPM-ALK
NPM-ALK^KD
NPM_tot-ALK
Number of colonies
***
g
Ba/F3
h
IL3 suspension
% cell viability
Time (d)
Ctrl
NPM-ALK
NPM-ALK^KD
NPM_tot-ALK

Figure 2

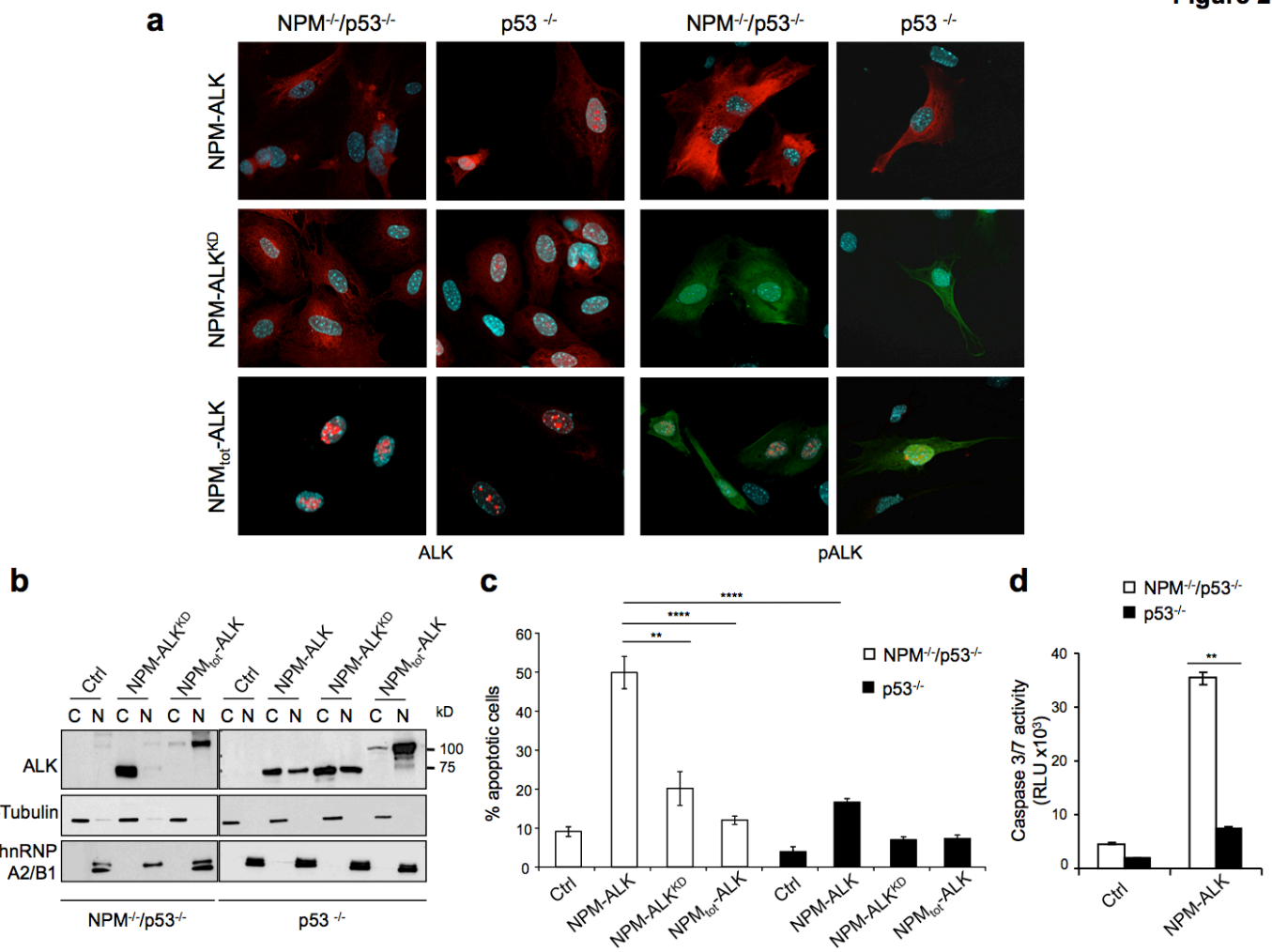
a
NPM-/-/p53-/-
p53 -/-
NPM-/-/p53-/-
p53 -/-
NPM-ALK
NPM-ALKKD
NPMtot-ALK
ALK
pALK
b
Ctrl
NPM-ALKKD
NPMtot-ALK
Ctrl
NPM-ALK
NPM-ALKKD
NPMtot-ALK
C N C N C N C N C N C N C N
kD
100
75
ALK
β-Tubulin
hnRNP A2/B1
NPM-/-/p53-/-
p53 -/-
c
% apoptotic cells
NPM-/-/p53-/-
p53-/-
****
****
**
Ctrl
NPM-ALK
NPM-ALKKD
NPMtot-ALK
Ctrl
NPM-ALK
NPM-ALKKD
NPMtot-ALK
d
NPM-/-/p53-/-
p53-/-
Caspase 3/7 activity (RLU x10³)
**
Ctrl
NPM-ALK

Figure 3

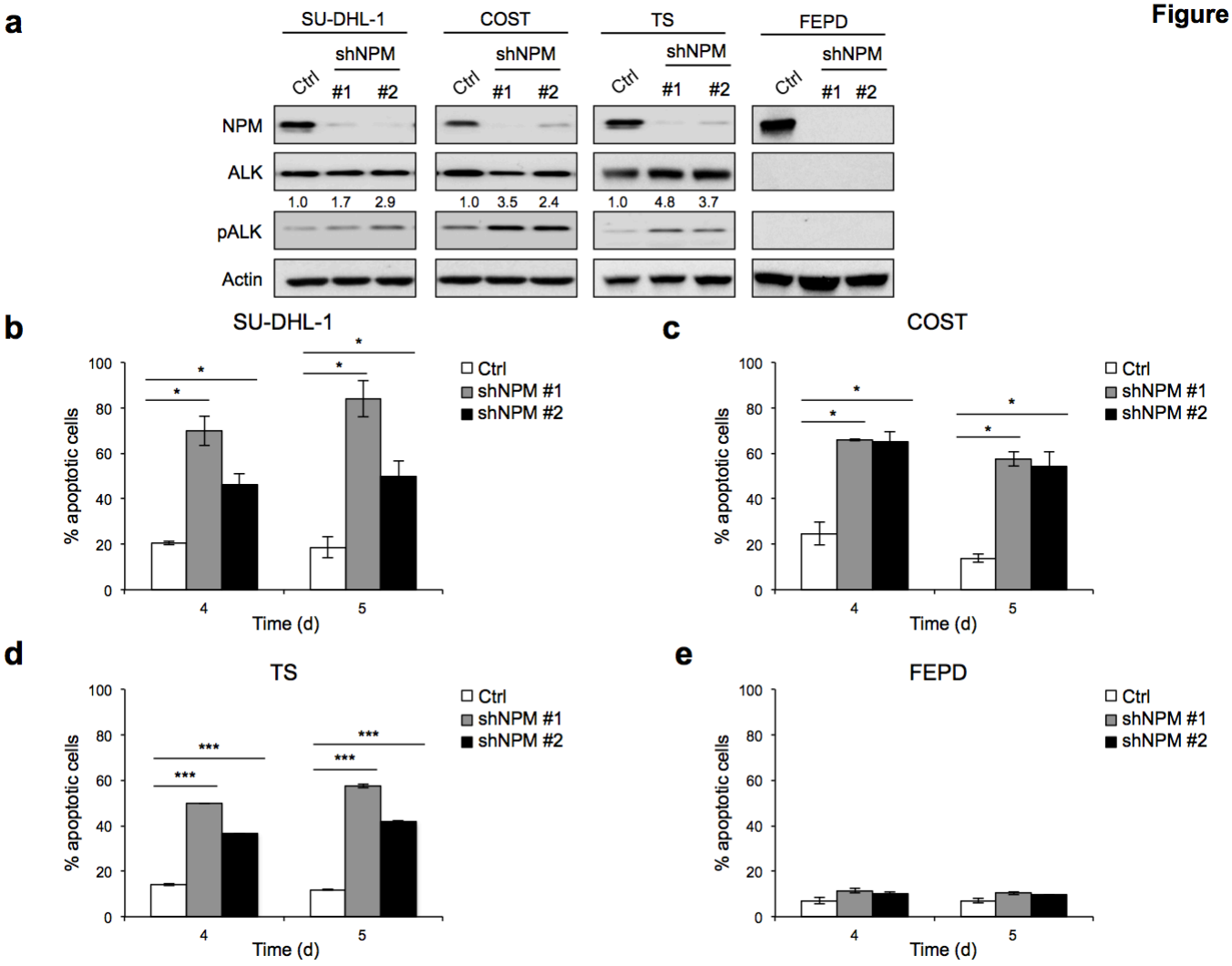
a
SU-DHL-1
COST
TS
FEPD
shNPM
Ctrl
#1
#2
NPM
ALK
1.0 1.7 2.9
1.0 3.5 2.4
1.0 4.8 3.7
pALK
Actin
b
SU-DHL-1
c
COST
d
TS
e
FEPD
% apoptotic cells
Time (d)
Ctrl
shNPM #1
shNPM #2

Figure 4

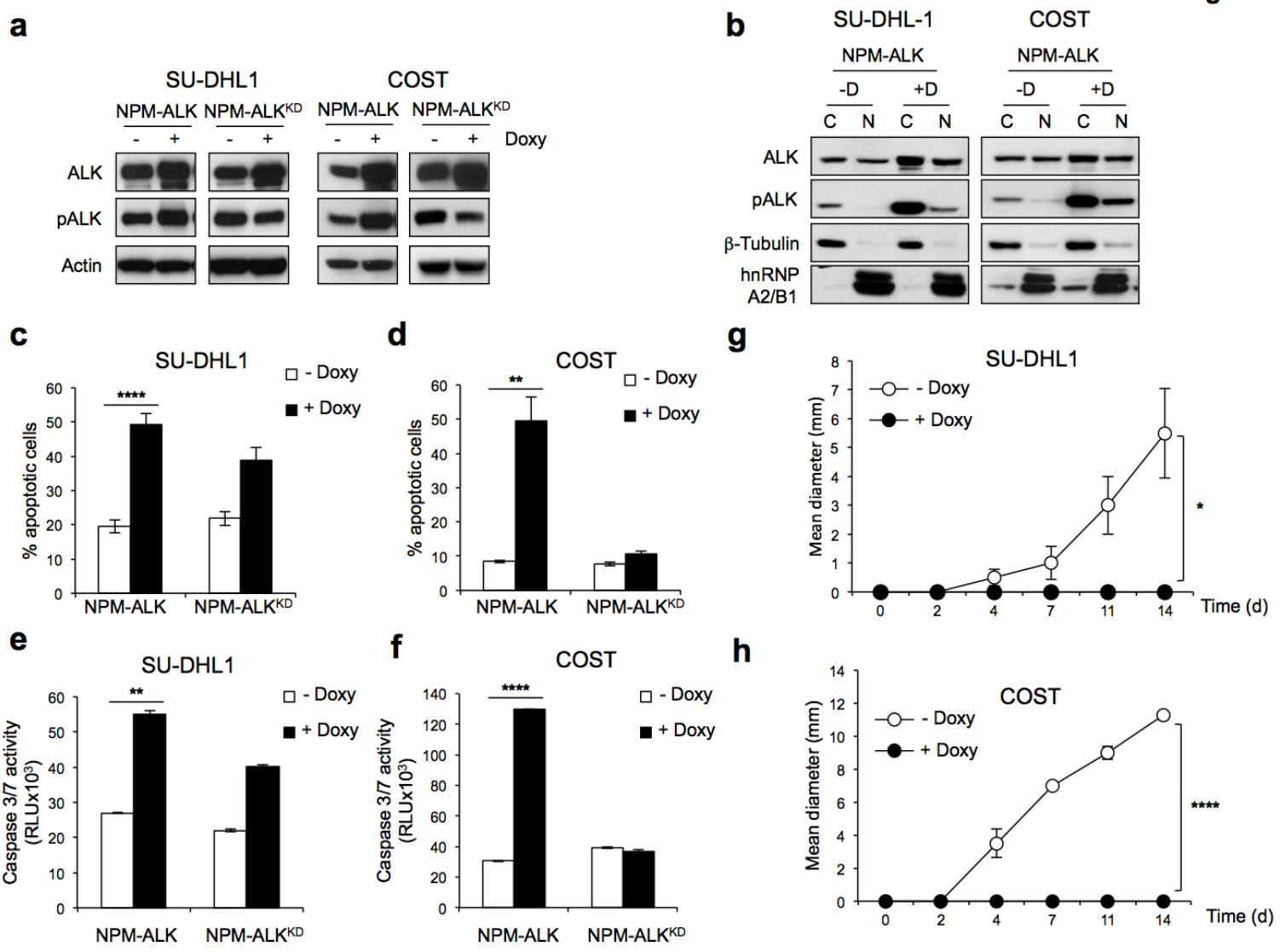
a
SU-DHL1
COST
NPM-ALK
NPM-ALK^KD
Doxy
ALK
pALK
Actin
b
SU-DHL-1
COST
NPM-ALK
-D
+D
C
N
ALK
pALK
β-Tubulin
hnRNP A2/B1
c
SU-DHL1
- Doxy
+ Doxy
% apoptotic cells
****
NPM-ALK
NPM-ALK^KD
d
COST
**
e
SU-DHL1
Caspase 3/7 activity (RLUx10^3)
f
COST
****
g
SU-DHL1
Mean diameter (mm)
Time (d)
*
h
COST
****

Figure 5

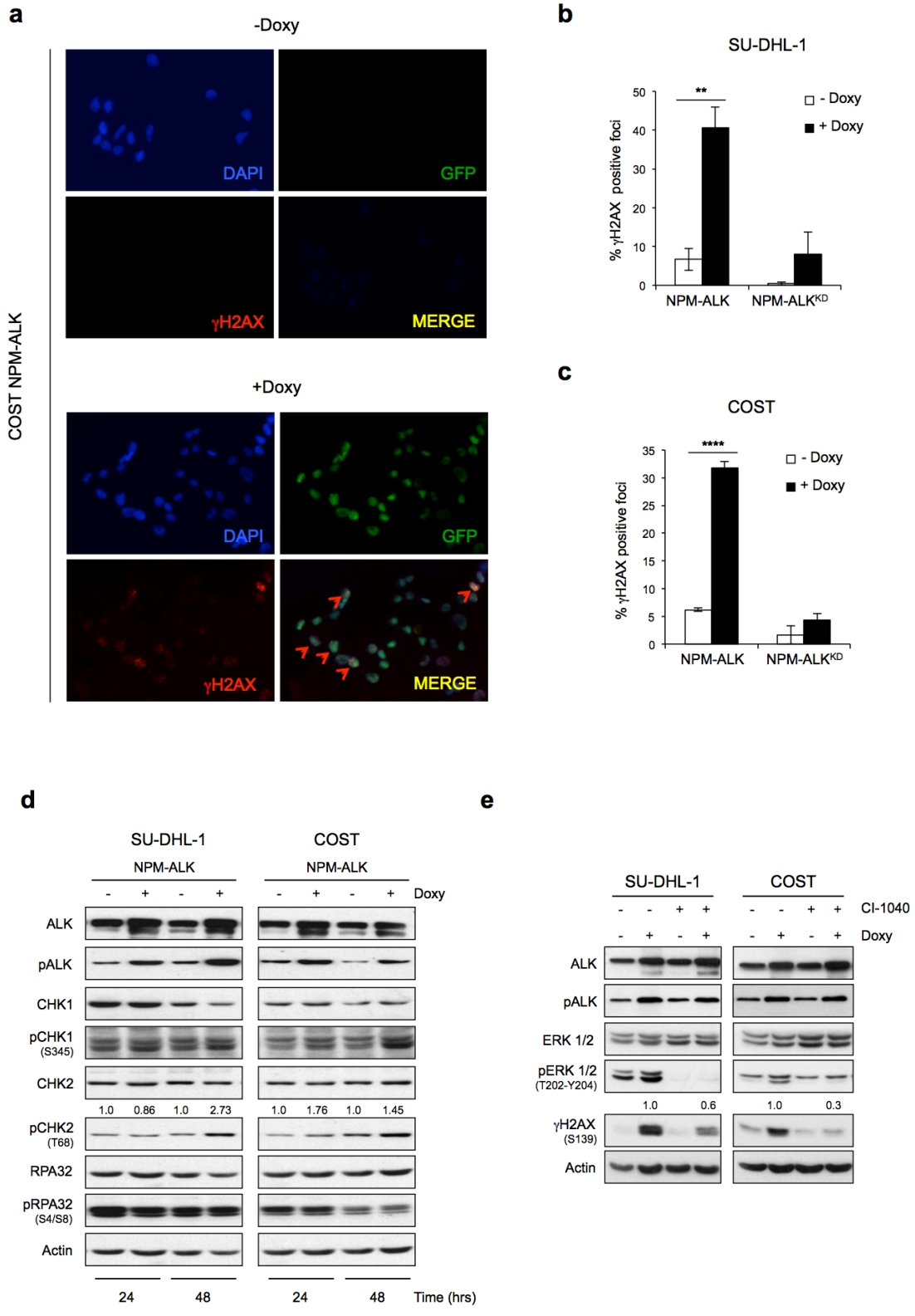
a
-Doxy
+Doxy
COST NPM-ALK
DAPI
GFP
γH2AX
MERGE
b
SU-DHL-1
**
- Doxy
+ Doxy
% γH2AX positive foci
NPM-ALK
NPM-ALK^KD
c
COST
****
- Doxy
+ Doxy
% γH2AX positive foci
NPM-ALK
NPM-ALK^KD
d
SU-DHL-1
COST
NPM-ALK
Doxy
ALK
pALK
CHK1
pCHK1 (S345)
CHK2
1.0 0.86 1.0 2.73
1.0 1.76 1.0 1.45
pCHK2 (T68)
RPA32
pRPA32 (S4/S8)
Actin
24 48 24 48 Time (hrs)
e
SU-DHL-1
COST
CI-1040
Doxy
ALK
pALK
ERK 1/2
pERK 1/2 (T202-Y204)
1.0 0.6 1.0 0.3
γH2AX (S139)
Actin

Figure 6

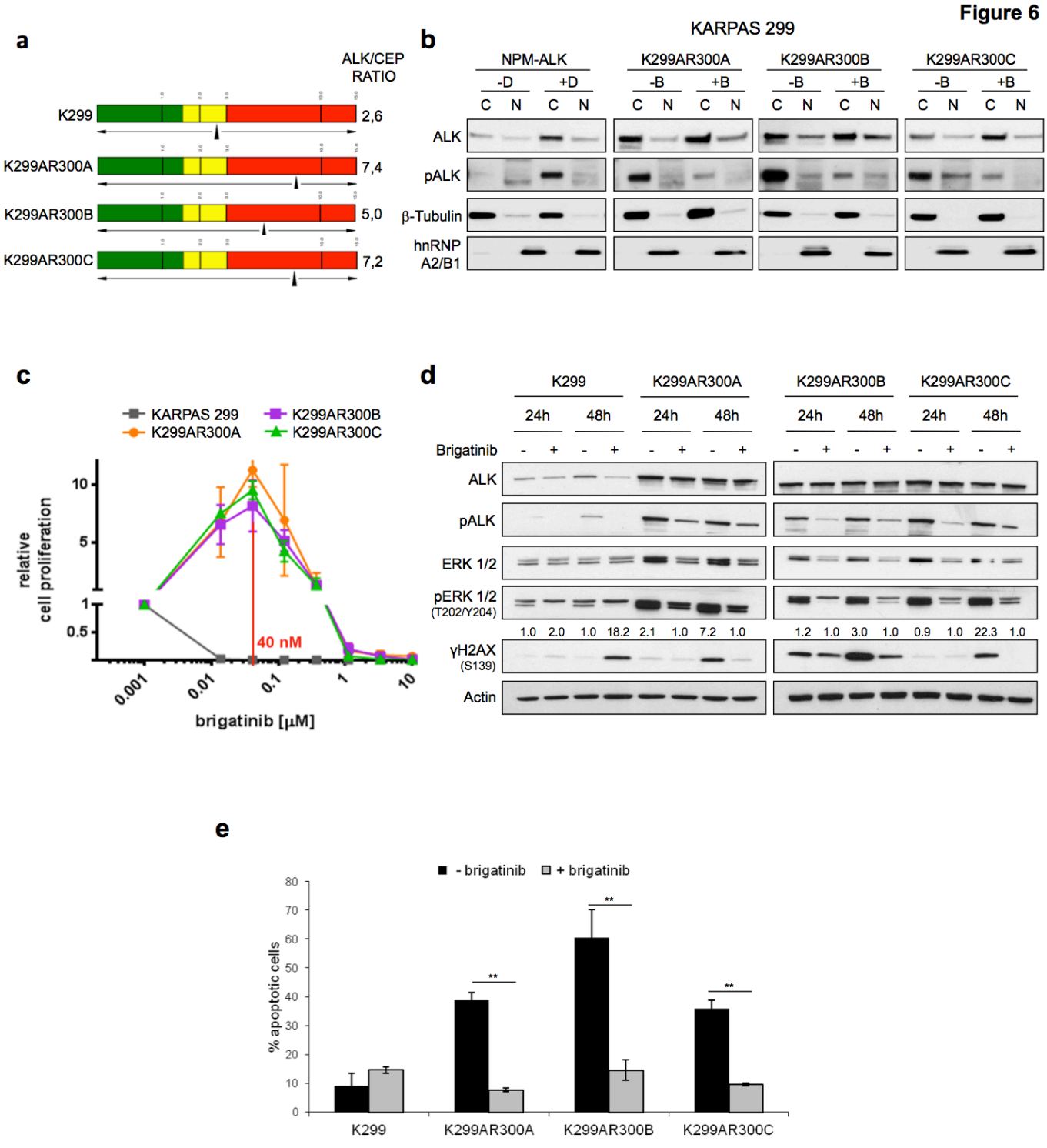
a
ALK/CEP RATIO
K299
2,6
K299AR300A
7,4
K299AR300B
5,0
K299AR300C
7,2
b
KARPAS 299
NPM-ALK
K299AR300A
K299AR300B
K299AR300C
-D
+D
-B
+B
C N
ALK
pALK
β-Tubulin
hnRNP A2/B1
c
KARPAS 299
K299AR300A
K299AR300B
K299AR300C
relative cell proliferation
40 nM
brigatinib [μM]
d
K299
K299AR300A
K299AR300B
K299AR300C
24h
48h
Brigatinib
ALK
pALK
ERK 1/2
pERK 1/2 (T202/Y204)
1.0 2.0 1.0 18.2 2.1 1.0 7.2 1.0
1.2 1.0 3.0 1.0 0.9 1.0 22.3 1.0
γH2AX (S139)
Actin
e
- brigatinib
+ brigatinib
% apoptotic cells
K299
K299AR300A
K299AR300B
K299AR300C

Figure 7

a

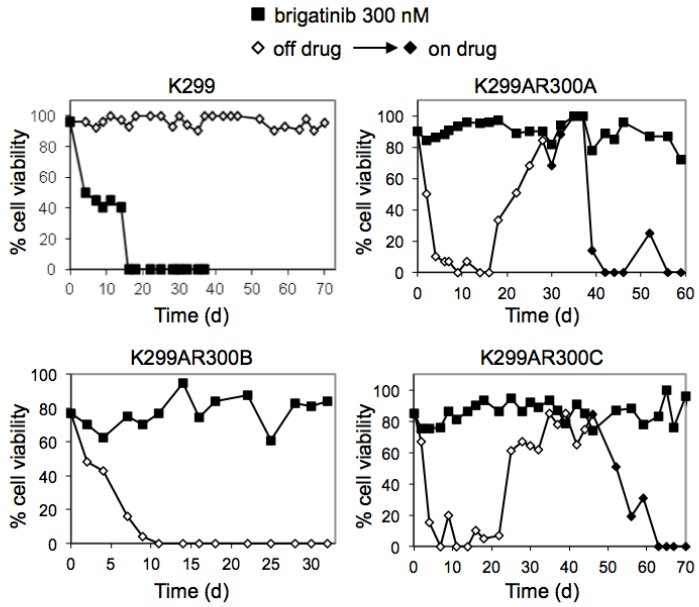

b

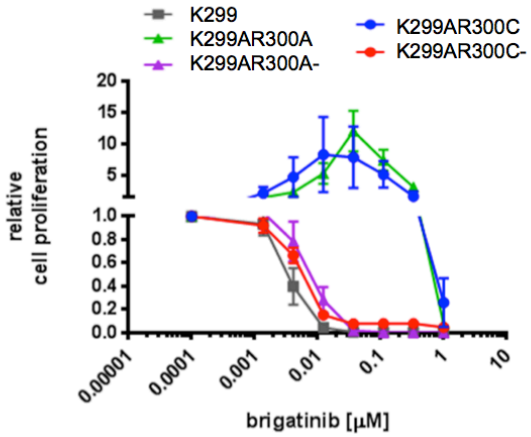

c

	IC_{50}	RR index
K299	0.003	1
K299AR300A	0.283	91
K299AR300A-	0.007	2.3
K299AR300C	0.250	80
K299AR300C-	0.006	1.9

RR < 2 | RR=2.1-4 | RR = 4.1-10 | RR > 10

d

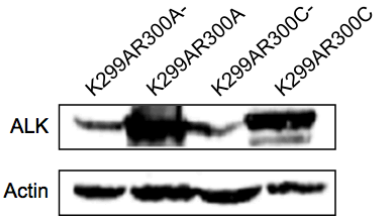

Figure 8

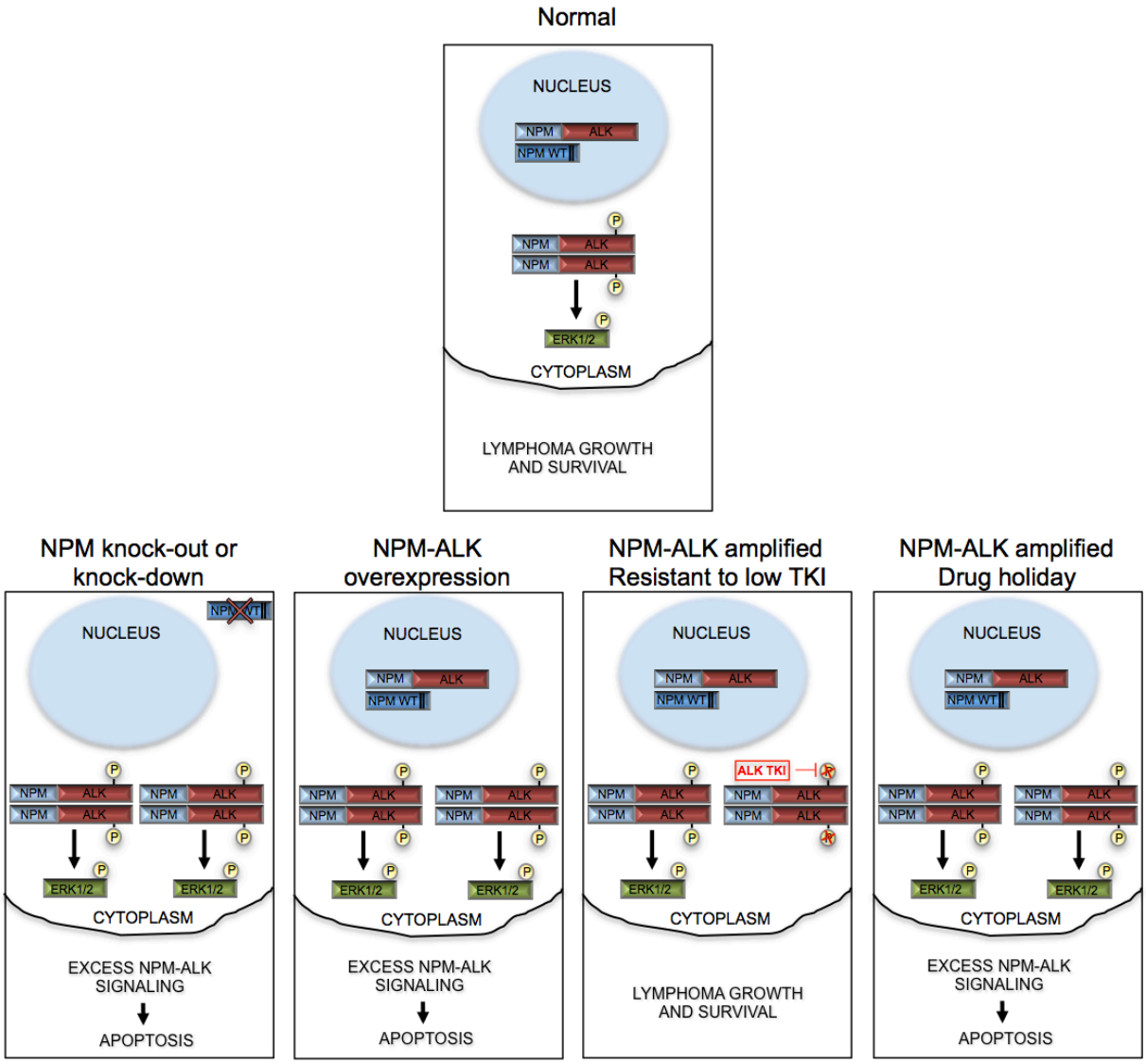
Normal
NUCLEUS
NPM
ALK
NPM WT
P
ERK1/2
CYTOPLASM
LYMPHOMA GROWTH
AND SURVIVAL
NPM knock-out or
knock-down
NPM WT
EXCESS NPM-ALK
SIGNALING
APOPTOSIS
NPM-ALK
overexpression
NPM-ALK amplified
Resistant to low TKI
ALK TKI
NPM-ALK amplified
Drug holiday